ChemInform Abstract: 3D Microporous Base-Functionalized Covalent Organic Frameworks for Size-Selective Catalysis.

ARTICLE *in* ANGEWANDTE CHEMIE INTERNATIONAL EDITION · MARCH 2014

Impact Factor: 11.26 · DOI: 10.1002/anie.201310500 · Source: PubMed

6 AUTHORS, INCLUDING:

Shuang Gu
University of Delaware
50 PUBLICATIONS **1,082** CITATIONS
SEE PROFILE

Zhongbin Zhuang
Beijing University of Chemical Technology
26 PUBLICATIONS **1,071** CITATIONS
SEE PROFILE

Shilun Qiu
Jilin University
258 PUBLICATIONS **7,611** CITATIONS
SEE PROFILE

Yushan Yan
University of Delaware
245 PUBLICATIONS **8,774** CITATIONS
SEE PROFILE

Covalent Organic Frameworks

DOI: 10.1002/anie.201310500

3D Microporous Base-Functionalized Covalent Organic Frameworks for Size-Selective Catalysis

*Qianrong Fang, Shuang Gu, Jie Zheng, Zhongbin Zhuang, Shilun Qiu, and Yushan Yan**

Abstract: *The design and synthesis of 3D covalent organic frameworks (COFs) have been considered a challenge, and the demonstrated applications of 3D COFs have so far been limited to gas adsorption. Herein we describe the design and synthesis of two new 3D microporous base-functionalized COFs, termed BF-COF-1 and BF-COF-2, by the use of a tetrahedral alkyl amine, 1,3,5,7-tetraaminoadamantane (TAA), combined with 1,3,5-triformylbenzene (TFB) or triformylphloroglucinol (TFP). As catalysts, both BF-COFs showed remarkable conversion (96 % for BF-COF-1 and 98 % for BF-COF-2), high size selectivity, and good recyclability in base-catalyzed Knoevenagel condensation reactions. This study suggests that porous functionalized 3D COFs could be a promising new class of shape-selective catalysts.*

Covalent organic frameworks (COFs)[1] are an emerging class of porous crystalline polymers with potential applications in gas adsorption[2] and optoelectronics.[3] COFs are composed of light elements, typically H, B, C, N, and O, which crystallize into periodic two-dimensional (2D) layers or three-dimensional (3D) networks by the formation of strong covalent bonds. The synthesis and properties of 2D COFs with layered eclipsed structures have been relatively well established.[4] A 2D imine-based COF loaded with Pd ions (in its pores) through a coordination reaction between nitrogen atoms in the framework and Pd ions to afford Pd/COF-LZU1 exhibited excellent catalytic activity in the Suzuki–Miyaura Coupling reaction.[5] By contrast, the design, preparation, and structural solution of 3D COFs are still considered to be a great challenge. In particular, despite their high surface areas ($>4000\ m^2 g^{-1}$) and record-low densities ($0.17\ g cm^{-3}$), these COFs with 3D networks have no well-developed applications, except for gas adsorption.[6]

In this study, two new 3D microporous base-functionalized COFs, termed BF-COF-1 and BF-COF-2 (Scheme 1), were designed and synthesized by combining tetrahedral and triangular building units in Schiff base reactions. Most importantly, because of their microporosity and basicity, both BF-COFs were studied for their catalytic performance in the Knoevenagel condensation reaction, and both BF-COFs showed remarkable conversion (96 % for BF-COF-1 and 98 % for BF-COF-2), high size selectivity, and good recyclability. To the best of our knowledge, no previous example of a 3D functionalized COF for catalysis has been reported.

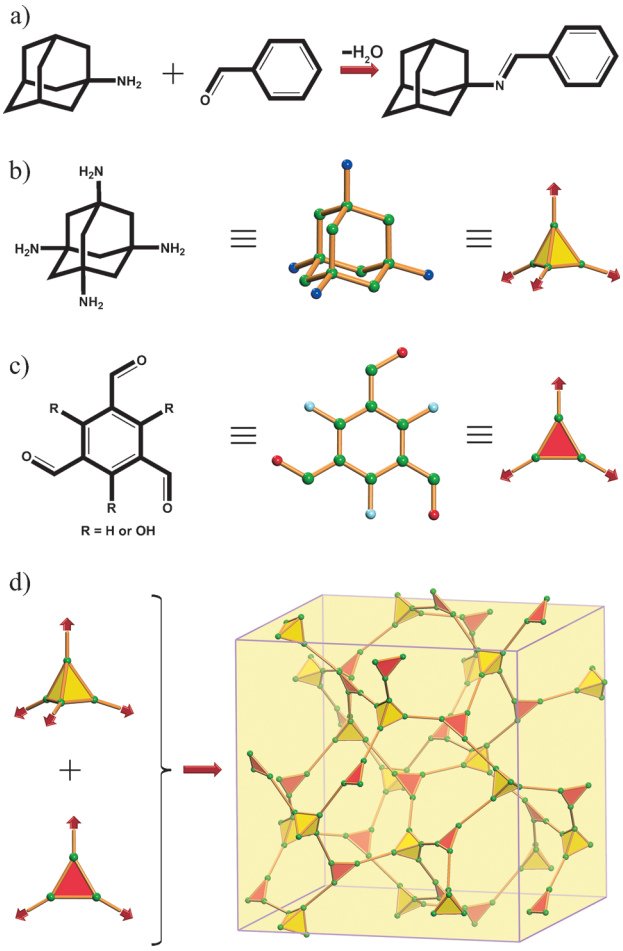

Scheme 1. Schematic representation of the strategy for preparing 3D microporous base-functionalized COFs. a) Model reaction of 1-adamantanamine with benzaldehyde to form the molecular *N*-(1-adamantyl)benzaldehyde imine. b) Structure of 1,3,5,7-tetraaminoadamantane (TAA) as a tetrahedral building unit. c) Structure of 1,3,5-triformylbenzene (R = H, TFB) or triformylphloroglucinol (R = OH, TFP) as a triangular building unit. d) Condensation of tetrahedral and triangular building units to give a 3D network with the symbol **ctn** (BF-COF-1 or BF-COF-2).

Our strategy for preparing 3D porous imine-based COFs involves the first use of a tetrahedral alkyl amine, 1,3,5,7-tetraaminoadamantane (TAA). The condensation of 1-ada-

[*] Dr. Q. Fang, Dr. S. Gu, J. Zheng, Dr. Z. Zhuang, Prof. Dr. Y. S. Yan
Department of Chemical and Biomolecular Engineering
Center for Catalytic Science and Technology, University of Delaware
Newark, DE 19716 (USA)
E-mail: yanys@udel.edu
Prof. S. Qiu
State Key Laboratory of Inorganic Synthesis and Preparative Chemistry, Jilin University
Changchun 130012 (China)

Supporting information for this article is available on the WWW under http://dx.doi.org/10.1002/anie.201310500.

mantanamine with benzaldehyde resulted in imine-bond formation with the elimination of water (Scheme 1a), as verified by ^{1}H NMR spectroscopy (see Figure S1 in the Supporting Information). The alkyl amine 1-adamatanamine has stronger basicity ($pK_a = 10.76$, calculated by using ACD/Labs Software V11.02, Chemical Abstracts Service, as hereinafter) than aromatic amines (aniline, $pK_a = 4.61$), and thus its product, *N*-(1-adamantyl)benzaldehyde imine, also shows stronger basicity ($pK_a = 6.26$) than that of *N*-benzylideneaniline ($pK_a = 3.23$),[6b] which suggests that imine-based COFs constructed from alkyl amines could be more promising base catalysts. However, such 3D COFs have never been reported so far. In this study, adamantane was substituted with four amine groups to form a tetrahedral alkyl amine, TAA, as an ideal four-connected building unit (Scheme 1b). Notably, TAA is superior to flexible four-connected alkyl amines (such as tetrakis(aminomethyl)methane), because its tetrahedral form can be entirely maintained during the reaction. As the aldehyde reaction partner, benzaldehyde was extended to 1,3,5-triformylbenzene (TFB) or triformylphloroglucinol (TFP) to act as the planar triangular building unit (Scheme 1c). Condensation reactions between tetrahedral TAA and triangular TFB or TFP could give novel 3D porous functionalized COFs through imine-bond formation. In the present case, the most likely net is **ctn** (Scheme 1d).[7]

BF-COFs were synthesized by solvothermolysis of a suspension of TAA and TFB or TFP in a 10:1 (v/v) mixture of mesitylene and 3 M aqueous acetic acid, followed by heating at 120 °C for 5 days, to give a crystalline solid in 82% yield for BF-COF-1 and 80% yield for BF-COF-2. These products were insoluble in water or common organic solvents, such as acetone, ethanol, hexanes, *N*,*N*-dimethylformamide (DMF), and tetrahydrofuran (THF). Scanning electron microscopy (SEM) images showed that the BF-COFs crystallized with a uniform polyhedral morphology and a particle size of about 0.3 μm, thus suggesting their phase purity (Figure 1, insets). The Fourier transform infrared (FTIR) spectra of the BF-COFs indicated the disappearance of the carbonyl stretching band of TFB (1691 cm^{-1}) or TFP (1639 cm^{-1}) as well as the N–H stretching band of TAA (3100–3300 cm^{-1}). For BF-COF-1, a new characteristic stretching band of the imine (C=N) functional group (1635 cm^{-1}) was observed (see Figure S2). Unlike BF-COF-1, BF-COF-2 displayed strong peaks at 1613, 1579, and 1278 cm^{-1} arising from the C=O, C=C, and C–N stretching bands present in the keto form but not the enol form. These values are similar to those found for the reference compound 2,4,6-tris[(phenylamino)methylene]-cyclohexane-1,35-trione (1612, 1571, and 1274 cm^{-1}, respectively; see Figure S3).[8] This phenomenon of enol-to-keto tautomerization has been well verified in previously reported studies, and it does not affect the structures of COFs.[9] The ^{13}C cross-polarization magic-angle-spinning (CP/MAS) NMR spectrum further confirmed the enol-to-keto tautomerization in BF-COF-2, with the shift of the peaks of TFP (see Figure S5). Both BF-COFs displayed high thermal stability, up to 350 and 370 °C, respectively, as determined by thermogravimetric analysis (TGA; see Figures S6 and S7).

The crystallinity of the BF-COFs was confirmed by powder X-ray diffraction (PXRD) analysis (Figure 1). Both

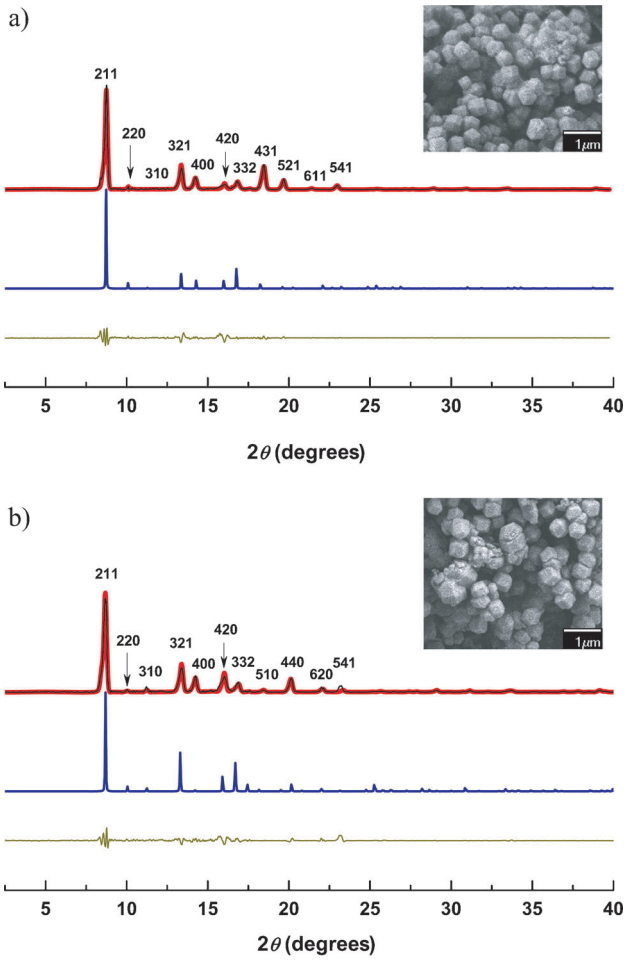

Figure 1. Powder XRD patterns of a) BF-COF-1 and b) BF-COF-2. The observed XRD patterns are shown in black, the refined patterns in red, the patterns calculated on the basis of the **ctn** net in blue, and the difference between the observed and refined profiles (observed−refined) in olive green. SEM images of the BF-COFs are also shown.

BF-COFs exhibited an intense peak at 8.7° corresponding to the reflection from the (211) plane. Extended structures based on a **ctn** net in the space group $I\bar{4}3d$ (no. 220) were modeled for both BF-COFs by using the Materials Studio software package.[10] After geometrical energy minimization by using the universal force field to optimize the geometry of the molecular building blocks, the unit-cell parameters and simulated PXRD patterns of both BF-COFs were obtained. Excellent agreement between the experimental and simulated PXRD patterns was observed for both BF-COFs (Figure 1). Also, the full-profile pattern-matching (Pawley) refinements based on their experimental PXRD patterns were calculated, and unit-cell parameters nearly equivalent to those determined from the models were found, with good agreement factors of $wR_p = 9.63\%$ and $R_p = 6.21\%$ for BF-COF-1 and $wR_p = 9.72\%$ and $R_p = 6.35\%$ for BF-COF-2. PXRD patterns were also calculated for the BF-COFs on the basis of **bor** net; in both cases, the calculated pattern did not match the experimental PXRD pattern (see Figures S8–S13). On the basis of these results, both BF-COFs were proposed to have the expected architectures with the **ctn** net. BF-COF-

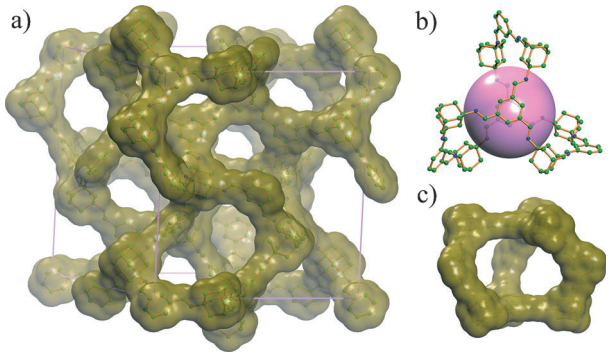

Figure 2. Extended structure of BF-COF-1. a) Atomic connectivity in BF-COF-1 with atom surfaces in olive green. Carbon and nitrogen are represented as green and blue spheres, respectively. b) A microporous cavity (pink sphere) with a diameter of 7.8 Å in BF-COF-1. c) Rectangular windows with a diameter of 7.8×11.3 Å^2 in BF-COF-1.

1 has microporous cavities with a diameter of 7.8 Å and rectangular windows with a size of 7.8×11.3 Å^2 (Figure 2), whereas BF-COF-2 exhibits microporous cavities of 7.7 Å with rectangular windows of 7.7×10.5 Å^2 (see Figures S14 and S15).

The permanent porosity of the BF-COFs was determined by measuring nitrogen-gas (N_2) adsorption at 77 K. Both BF-COFs exhibited the classic type I isotherms characterized by a sharp uptake under low relative pressures in the range of $P/P_0 = 10^{-5}$–10^{-2} (Figure 3), which is a signature feature of microporous materials. The lack of hysteresis indicates that the adsorption and desorption mechanisms are similar and that the adsorption is reversible. The Brunauer–Emmett–Teller (BET) surface areas of the BF-COFs were found to be 730 $m^2 g^{-1}$ for BF-COF-1 and 680 $m^2 g^{-1}$ for BF-COF-2 (see Figures S16 and S17). Both BF-COFs had relatively high Langmuir surface areas: 1028 $m^2 g^{-1}$ for BF-COF-1 and 974 $m^2 g^{-1}$ for BF-COF-2 (see Figures S18 and S19). The total pore volumes were evaluated at $P/P_0 = 0.90$ to be $V_p = 0.43$ $cm^3 g^{-1}$ for BF-COF-1 and 0.39 $cm^3 g^{-1}$ for BF-COF-2. The pore-size distributions of the BF-COFs were calculated on the basis of nonlocal density functional theory (NLDFT). Both BF-COFs showed a narrow pore width (8.3 Å for BF-COF-1 and 8.1 Å for BF-COF-2; Figure 3, insets), which was in agreement with the pore size predicted from the crystal structures (7.8 Å for BF-COF-1 and 7.7 Å for BF-COF-2).

To characterize their base properties, we studied both BF-COFs as catalysts for the Knoevenagel condensation reaction. The Knoevenagel condensation reaction is well-known, not only as a base-catalyzed model reaction but also as an important C–C bond-forming reaction in organic synthesis for the preparation of coumarins and their derivatives, which are important intermediates in the synthesis of cosmetics, perfumes, and pharmaceuticals.[11] To demonstrate the catalytic activity and size selectivity of the BF-COFs, substrates with different sizes were employed: benzaldehyde (6.1×8.7 Å^2), 4-methylbenzaldehyde (6.1×10.1 Å^2), 4-phenylbenzaldehyde (6.1×13.3 Å^2), 4-(4-methylphenyl)benzaldehyde (6.1×14.7 Å^2), and malononitrile (4.5×6.9 Å^2; Scheme 2; the size of reactants was calculated as the longest distance of these molecules in two perpendicular directions).

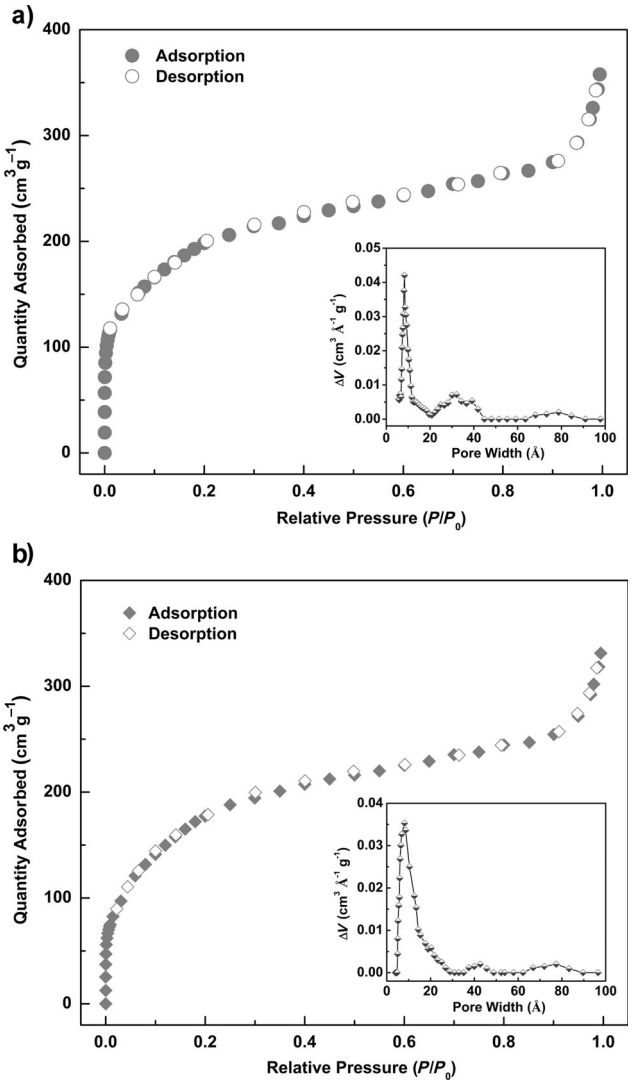

Figure 3. Nitrogen-gas adsorption (filled symbols) and desorption isotherms (open symbols) measured at 77 K for a) BF-COF-1 and b) BF-COF-2. Inset: Pore-size distribution of the BF-COFs, as calculated by fitting NLDFT models to the adsorption data.

Typically, the Knoevenagel reaction was performed with 1 mmol of each substrate in benzene (6 mL) with BF-COF-1 or BF-COF-2 (5 mol%) for 10 h at room temperature. The conversion of the reaction was detected by ^{1}H NMR spectroscopy as based on the starting materials (see Figures S20–S27). After the reactions, the BF-COFs remained unchanged in terms of weight, color, and morphology (see Figures S28 and S29). The results of PXRD and N_2 adsorption further confirmed the structural integrity of the BF-COFs after catalytic tests, thus suggesting the high stability of these COF materials in the Knoevenagel reaction (see Figures S30–S33). Furthermore, for heterogeneous catalysts, these COF materials can be readily isolated from the reaction suspension by a simple filtration and reused almost without loss of activity at least three times (see Figures S34 and S35).

The molecular sizes of the products are shown in Table S5 in the Supporting Information. The product of reaction I (7.6×10.4 Å^2) is smaller than the windows of the BF-COFs

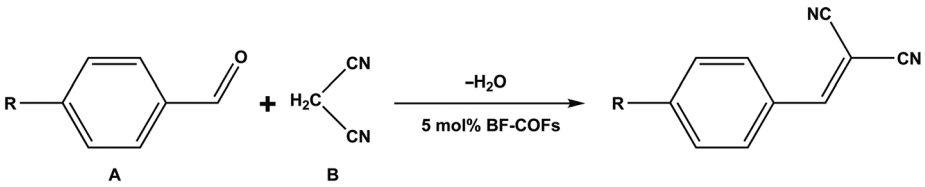

Reaction	A	B	Catalyst	Conversion (%)
I	8.7 Å × 6.1 Å	6.9 Å × 4.5 Å	BF-COF-1	96
			BF-COF-2	98
II	10.1 Å × 6.1 Å	6.9 Å × 4.5 Å	BF-COF-1	4
			BF-COF-2	3
III	13.3 Å × 6.1 Å	6.9 Å × 4.5 Å	BF-COF-1	3
			BF-COF-2	4
IV	14.7 Å × 6.1 Å	6.9 Å × 4.5 Å	BF-COF-1	2
			BF-COF-2	2

Scheme 2. Catalytic activity of BF-COFs in the Knoevenagel condensation reaction.

(7.8×11.3 Å^2 for BF-COF-1 and 7.7×10.5 Å^2 for BF-COF-2); however, the products of reactions II–IV have a size of 7.6×12.2, 7.6×15.4, and 7.6×16.8 Å^2, respectively, and are thus larger than the windows of the BF-COFs. Reaction I proceeded with high conversion into the product (96% for BF-COF-1 and 98% for BF-COF-2; Scheme 2 and Figure 4), thus suggesting that the reaction occurred in the pores of the BF-COFs. On the contrary, reactions II–IV proceeded with about 2–4% conversion for both BF-COFs, which implied that they could not take place in the channels of the BF-COFs; alternatively, if the reactions occurred, their products were trapped in the pores, and no more reactions took place. The limited conversion of reactions II–IV probably occurred on the surface of the BF-COFs. For comparison, catalytic reactions with small-molecule catalysts (1-adamantylamine, *N*,*N*′,*N*″-(1,3,5-benzenetriyltrimethylidyne)triadamantylamine, and 2,4,6-tris((adamantylamino)methylene)cyclohexane-1,3,5-trione) were carried out under the same conditions; all of these catalysts showed high conversion (77–97%; see Figures S40–S47 and Table S6) with little selectivity, which confirmed that the BF-COFs are superior to these small molecules in terms of their size selectivity. To further investigate the selectivity of the BF-COFs, we carried out catalytic experiments with a mixture of the starting materials (benzaldehyde, 4-phenylbenzaldehyde, and malononitrile) for the Knoevenagel reaction. The results indicated that both BF-COFs exhibited excellent size selectivity associated with high conversion (97 versus 2% for BF-COF-1 and 97 versus 3% for BF-COF-2) and are consistent with the results of the single-reactant reactions (see Figures S48 and S49).

To the best of our knowledge, although base-functionalized zeolites and metal–organic frameworks (MOFs) have been studied for the Knoevenagel condensation reaction, reports on COFs have yet to appear.[12] COFs are crystalline porous organic materials that in general have a larger pore size and a higher surface area than those of zeolites as well as higher chemical stability than that of MOFs. Considering these desirable properties, COFs are a promising new class of catalysts that are expected to be superior to MOFs and zeolites. Furthermore, the differently sized reactants studied are typical substrates for the Knoevenagel condensation reaction, and the results confirmed the catalytic performance of the BF-COFs as a result of their basicity as well as their high selectivity due to their pore sizes. On the basis of these results, it is likely that other reactions can also be catalyzed and that these experiments will promote the application of COFs as selective catalysts.

In conclusion, we have synthesized two novel 3D microporous base-functionalized COFs, BF-COF-1 and BF-COF-2, by combining a tetrahedral alkyl amine, TAA, with planar triangular building units, TFB and TFP. On the basis of the characterization of their microporosity and basicity, the catalytic properties of the BF-COFs were explored in the Knoevenagel condensation reaction, and both BF-COFs were shown to have excellent catalytic activity with high conversion (96% for BF-COF-1 and 98% for BF-COF-2), highly efficient size selectivity, and good recyclability. It is believed that the 3D porous functionalized COFs successfully prepared in this study may not only inspire the synthesis of new 3D COFs with ideal building units, but also greatly facilitate the development of COFs as promising selective catalysts by their rational design with pores and windows of different sizes.

Received: December 4, 2013
Published online: February 7, 2014

Keywords: covalent organic frameworks · crystalline materials · functionalized materials · heterogeneous catalysis · porous materials

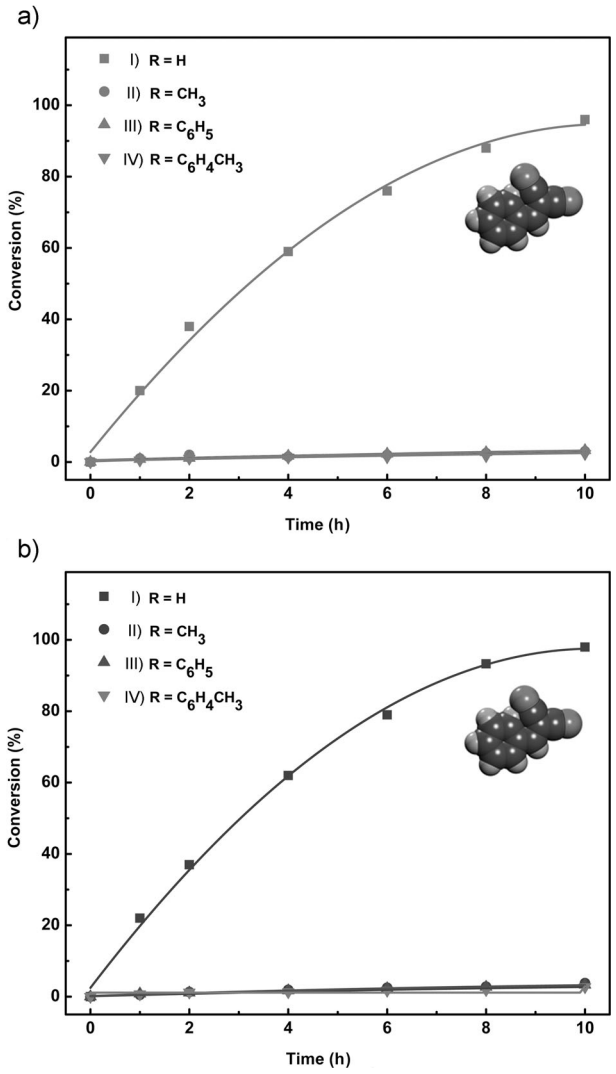

Figure 4. Conversion (%) versus time (h) for Knoevenagel condensation reactions in a) BF-COF-1 and b) BF-COF-2. Inset: Structure of the product formed from benzaldehyde and malononitrile.

[1] a) A. P. Côté, A. I. Benin, N. W. Ockwig, M. O'Keeffe, A. J. Matzger, O. M. Yaghi, *Science* **2005**, *310*, 1166 – 1170; b) J. W. Colson, A. R. Woll, A. Mukherjee, M. P. Levendorf, E. L. Spitler, V. B. Shields, M. G. Spencer, J. Park, W. R. Dichtel, *Science* **2011**, *332*, 228 – 231; c) X. Feng, X. S. Ding, D. L. Jiang, *Chem. Soc. Rev.* **2012**, *41*, 6010 – 6022; d) S. Y. Ding, W. Wang, *Chem. Soc. Rev.* **2013**, *42*, 548 – 568; e) Z. Xiang, D. Cao, *J. Mater. Chem. A* **2013**, *1*, 2691 – 2718.

[2] a) H. M. El-Kaderi, J. R. Hunt, J. L. Mendoza-Cortes, A. P. Côté, R. E. Taylor, M. O'Keeffe, O. M. Yaghi, *Science* **2007**, *316*, 268 – 272; b) J. L. Mendoza-Cortes, S. S. Han, H. Furukawa, O. M. Yaghi, W. A. Goddard III, *J. Phys. Chem. A* **2010**, *114*, 10824 – 10833; c) B. Assfour, G. Seifert, *Microporous Mesoporous Mater.* **2010**, *133*, 59 – 65; d) H. Furukawa, O. M. Yaghi, *J. Am. Chem. Soc.* **2009**, *131*, 8875 – 8883; e) S. S. Han, H. Furukawa, O. M. Yaghi, W. A. Goddard III, *J. Am. Chem. Soc.* **2008**, *130*, 11580 – 11581; f) R. Babarao, J. Jiang, *Energy Environ. Sci.* **2008**, *1*, 139 – 143; g) G. Garberoglio, *Langmuir* **2007**, *23*, 12154 – 12158; h) S. S. Han, J. L. Mendoza-Cortes, W. A. Goddard, *Chem. Soc. Rev.* **2009**, *38*, 1460 – 1476; i) Y. Li, R. T. Yang, *AICHE J.* **2008**, *54*, 269 – 279; j) J. L. Mendoza-Cortes, T. A. Pascal, W. A. Goddard III, *J. Phys. Chem. A* **2011**, *115*, 13852 – 13857; k) F. J. Uribe-Romo, C. J. Doonan, H. Furukawa, K. Oisaki, O. M. Yaghi, *J. Am. Chem. Soc.* **2011**, *133*, 11478 – 11481; l) M. G. Rabbani, A. K. Sekizkardes, Z. Kahveci, T. E. Reich, R. Ding, H. M. El-Kaderi, *Chem. Eur. J.* **2013**, *19*, 3324 – 3328.

[3] a) S. Wan, J. Guo, J. Kim, H. Ihee, D. Jiang, *Angew. Chem.* **2008**, *120*, 8958 – 8962; *Angew. Chem. Int. Ed.* **2008**, *47*, 8826 – 8830; b) E. L. Spitler, W. R. Dichtel, *Nat. Chem.* **2010**, *2*, 672 – 677; c) S. Wan, J. Guo, J. Kim, H. Ihee, D. Jiang, *Angew. Chem.* **2009**, *121*, 5547 – 5550; *Angew. Chem. Int. Ed.* **2009**, *48*, 5439 – 5442; d) X. Ding, J. Guo, X. Feng, Y. Honsho, J. Guo, S. Seki, P. Maitarad, A. Saeki, S. Nagase, D. Jiang, *Angew. Chem.* **2011**, *123*, 1325 – 1329; *Angew. Chem. Int. Ed.* **2011**, *50*, 1289 – 1293; e) X. S. Ding, L. Chen, Y. Honsho, X. Feng, O. Saenpawang, J. D. Guo, A. Saeki, S. Seki, S. Irle, S. Nagase, V. Parasuk, D. L. Jiang, *J. Am. Chem. Soc.* **2011**, *133*, 14510 – 14513; f) S. Wan, F. Gandara, A. Asano, H. Furukawa, A. Saeki, S. K. Dey, L. Liao, M. W. Ambrogio, Y. Y. Botros, X. Duan, S. Seki, J. F. Stoddart, O. M. Yaghi, *Chem. Mater.* **2011**, *23*, 4094 – 4097; g) S. Patwardhan, A. A. Kocherzhenko, F. C. Grozema, L. D. A. Siebbeles, *J. Phys. Chem. C* **2011**, *115*, 11768 – 11772; h) X. Feng, L. Liu, Y. Honsho, A. Saeki, S. Seki, S. Irle, Y. Dong, A. Nagai, D. Jiang, *Angew. Chem.* **2012**, *124*, 2672 – 2676; *Angew. Chem. Int. Ed.* **2012**, *51*, 2618 – 2622; i) S. Jin, X. Ding, X. Feng, M. Supur, K. Furukawa, S. Takahashi, M. Addicoat, M. E. El-Khouly, T. Nakamura, S. Irle, S. Fukuzumi, A. Nagai, D. Jiang, *Angew. Chem.* **2013**, *125*, 2071 – 2075; *Angew. Chem. Int. Ed.* **2013**, *52*, 2017 – 2021; j) M. Dogru, M. Handloser, F. Auras, T. Kunz, D. Medina, A. Hartschuh, P. Knochel, T. Bein, *Angew. Chem.* **2013**, *125*, 2992 – 2996; *Angew. Chem. Int. Ed.* **2013**, *52*, 2920 – 2924; k) G. H. V. Bertrand, V. K. Michaelis, T.-C. Ong, R. G. Griffin, M. Dinca, *Proc. Natl. Acad. Sci. USA* **2013**, *110*, 4923 – 4928.

[4] J. W. Colson, W. R. Dichtel, *Nat. Chem.* **2013**, *5*, 453 – 465.

[5] S. Y. Ding, J. Gao, Q. Wang, Y. Zhang, W. G. Song, C. Y. Su, W. Wang, *J. Am. Chem. Soc.* **2011**, *133*, 19816 – 19822.

[6] a) J. R. Hunt, C. J. Doonan, J. D. LeVangie, A. P. Côté, O. M. Yaghi, *J. Am. Chem. Soc.* **2008**, *130*, 11872 – 11873; b) F. J. Uribe-Romo, J. R. Hunt, H. Furukawa, C. Klöck, M. O'Keeffe, O. M. Yaghi, *J. Am. Chem. Soc.* **2009**, *131*, 4570 – 4571; c) D. N. Bunck, W. R. Dichtel, *Angew. Chem.* **2012**, *124*, 1921 – 1925; *Angew. Chem. Int. Ed.* **2012**, *51*, 1885 – 1889; d) D. N. Bunck, W. R. Dichtel, *Chem. Commun.* **2013**, *49*, 2457 – 2459.

[7] O. Delgado-Friedrichs, M. O'Keeffe, O. M. Yaghi, *Acta Crystallogr. Sect. A* **2006**, *62*, 350 – 355.

[8] S. Kandambeth, A. Mallick, B. Lukose, M. V. Mane, T. Heine, R. Banerjee, *J. Am. Chem. Soc.* **2012**, *134*, 19524 – 19527.

[9] B. P. Biswal, S. Chandra, S. Kandambeth, B. Lukose, T. Heine, R. Banerjeet, *J. Am. Chem. Soc.* **2013**, *135*, 5328 – 5331.

[10] Materials Studio (Accelrys Inc., San Diego, CA).

[11] a) E. Knoevenagel, *Ber. Dtsch. Chem. Ges.* **1898**, *31*, 2585 – 2596; b) G. Jones, *Org. React.* **1967**, *15*, 204 – 599; c) F. Bigi, L. Chesini, R. Maggi, G. Sartori, *J. Org. Chem.* **1999**, *64*, 1033 – 1035; d) N. Yu, J. M. Aramini, M. W. Germann, Z. Huang, *Tetrahedron Lett.* **2000**, *41*, 6993 – 6996.

[12] a) A. Corma, V. Fornés, R. M. Martín-Aranda, H. García, J. Primo, *Appl. Catal.* **1990**, *59*, 237 – 248; b) J. Caro, M. Noack, *Microporous Mesoporous Mater.* **2008**, *115*, 215 – 233; c) S. Hasegawa, S. Horike, R. Matsuda, S. Furukawa, K. Mochizuki, Y. Kinoshita, S. Kitagawa, *J. Am. Chem. Soc.* **2007**, *129*, 2607 – 2614; d) J. Gascon, U. Aktay, M. D. Hernandez-Alonso, G. P. M. van Klink, F. Kapteijn, *J. Catal.* **2009**, *261*, 75 – 87.

